Experiment 6: Measurements on a Torsional Pendulum

Alex Garcia
Partners: Daniel Kaputa, Jacob Fritchie, and Gregory Kane III
TA: Jordan Sickle
Data taken October 20 & 27, 2020

November 10, 2020

Abstract

In this lab, we experimenting with several different types of oscillations of a torsional pendulum. We conduct several experiments with and without a driving motor. In either case, we are comparing our data to the solutions of a differential equation, the difference between driven and not is the homogeneity of this differential equation. In the first experiment we performed with no driving motor we attached a wire to the side of the pendulum and hung some masses from it. We found the torsional constant of the pendulum can be derived from the linear relationship between the mass and the displacement from equilibrium. In addition, from this torsional constant, we were able to match the shear constant of the wires to a handbook value. Our second experiment studied the free oscillation of our pendulum in order to determine the natural frequency from this compare to our torsional constant from the first experiment. We found decently good agreement between those two values. For the next three experiments, we looked at different damping types: viscous (magnetic), Coulomb, and turbulent. For each of these damped oscillations, we found good agreement with our differential equation's solutions for each of their respective damping terms. In addition, we were able to look at each system's logarithmic decrement and found each of the expected forms: exponential for viscous and turbulent and linear for Coulomb. At this juncture, we turned on the motor to drive our system. The first experiment with the motor examined the effect of driving the system at a frequency some large fraction of the natural frequency to examine the beat frequency. We found the form of the solution agreed with our expected oscillations with an oscillating envelope as well as a very close relation to our expected beat frequency. In the next part of the experiment, we wanted to know more about our system as a function of frequency. We drove the motor at several different frequencies and found the systems amplitude and phase difference between the motor and disk. We found functional forms that followed very closely with the theoretical models described in the Theory section. Finally, we ran the motor at half of the resonant frequency and found the frequency responses of the sub-harmonics. The frequencies we got out matched vary well with our expected values for the resonant and harmonic frequencies. Overall, we saw a very good relationship between our theoretical solutions to the differential equations and our data. In the future, more accurately measuring the properties of our system would help us achieve better fits and calculations for parameters. As well as, for the first two exercises with motors, using a more fine sweep of the frequencies (especially around the resonant frequency) would be more helpful.

1 Purpose

The purpose of this lab is exploring the solutions to our particular differential equation, for most of the experiments it is linear (the one experiment where it will be non-linear is Coulomb damping §3.5). For all of the cases where we have no driving motor the differential equation will be homogeneous. In fact, for the first two experiments the differential equation will not even have a damping term. The first of these two experiments was we attached a wire with a range of masses to the end and measured the displacement of the pendulum. The relationship between those two is going to be linear with the slope depending on the torsional constant. The torsional constant for the pendulum allows us to solve for two more values: the shear modulus of the wires and the natural frequency of the system. The second homogeneous, non-damped experiment was we just took our pendulum and perturbed it and watch it oscillate. From this oscillation we can fit a sine curve and find the natural frequency and compare it to the one we obtained in the first experiment.

Additionally, since we have the natural frequency, we can work backwards to obtain the torsional constant and compare with experiment one.

The next section of the lab focused a lot of the damping. We still have a homogeneous differential equation, but now we have some term proportional to the first derivative of displacement. We studied three different types of damping: viscous, coulomb and turbulent damping. The difference between all of these was the power of the derivative. Coulomb damping had only a dependence on the sign of the velocity. We institute Coulomb damping by having a paintbrush run along the side of the disk as it rotates. This damping should produce a decay on the system with a linear 'decay envelope'. The next type of damping is viscous which has a damping term proportional to the velocity. We created viscous damping by placing a large physical magnet around the disk. This magnet caused the system to decay in an exponential fashion. Finally, we looked at the non-linear damping, turbulent damping. The particular case we examined, that of taping Styrofoam orthogonal to the disk, was proportional to the velocity squared. This causes the envelope of the decay to be such that the log decrement is linear, not constant.

At this point we started using the motor and the differential equation became non-homogeneous. The first experiment we ran with the motor was to examine the beat frequency of running the motor at some frequency and measuring the response. We expect to see the oscillations follow some oscillating envelope, which has some relationship to the beat frequency (discussed further in Theory). The second experiment we conducted with the motor running was a sweep of several different frequencies to measure the response's amplitude and phase difference from the motor. Finally, we examined the sub-harmonics of the resonant frequency to demonstrate the small effect that a non-perfect sinusoidal motor has on our system.

2 Theory

Very similar to our studies of RLC circuits, the torsion pendulum follows a linear second-order differential equation. The form of this differential equation is shown below.

$$I\frac{d^2\theta}{dt^2} + K\theta + \tau_{\text{damping}} = \tau_{\text{ext}} \tag{2.1}$$

In this equation (Eqn. 2.1) the torque, τ_{damping}, comes from a motor driving our pendulum. In experiments 3.2 to 3.6 $\tau_{ext} = 0$ and thus we have a homogeneous differential equation. However, for the rest of the experiments this torque is non-zero.

Let us first consider the homogeneous case. The differential equation has two solutions with the following forms.

$$\theta_{1,2} = a \pm b \tag{2.2}$$

$$a = \frac{R}{2I}\ , \quad b = \sqrt{\left(\frac{R}{2I}\right)^2 - \frac{K}{I}} \tag{2.3}$$

These solutions yield three different forms. The first situation is where $b^2 > 0$, in this case the roots are real and the system is called over-damped. Over-damping the system will cause the oscillations to exponentially decay very rapidly. This is helpful in zeroing our pendulum, over-damp the disk with the magnet and it will rapidly stop rotating. The second form, where $b^2 = 0$, is called critically-damped. Critical-damping has the same form as over-damped, the only difference is that the decay happens much quicker. Finally we have $b^2 < 0$, this situation is known as under-damping. An under-damped pendulum will continue to oscillate around zero but it will have some decay.

The decay form will be characterized by the different type of damping. In our experiments we learn more about three different types of decay: viscous, coulomb and turbulent.

Viscous damping is caused by the magnet that we place around the rotating disk and is characterized by an exponential decay. Viscous damping has the following form for τ_{damping}.

$$\tau = C\dot{\theta} \tag{2.4}$$

We can describe the decay of peaks using the log decrement, δ, which is defined as follows.

$$\delta = \ln\left(\frac{\theta_{n+1}}{\theta_n}\right) = aT \tag{2.5}$$

In Origin, our data analysis software, we can fit this decay to a sine damp function and we know the following relation for the attenuation constant a based on the fits.

$$a = \frac{1}{t_0} \tag{2.6}$$

Similarly, we know that by Origin's fitting parameters the log decrement is defined as the following. (The w in this equation is addressed in Eqn. 2.28)

$$\delta = \frac{2w}{t_0} \tag{2.7}$$

The second type of damping we study is Coulomb damping. This exerts the damping torque of the following functional form.

$$\tau = C \operatorname{sgn}\dot{\theta} \tag{2.8}$$

We employ Coulomb damping with a small paint brush against the thick side of the disk. This brush provides the friction to slow down the disk's rotation (An interesting aside about this friction is that when the disk instantaneously becomes at rest when it is changing direction the friction force will be static friction. This will cause the disk to not fully return to its original zero position, but instead some small offset where the friction force is too large to overcome). Coulomb damping will create a linear decay, this has the following slope.

$$\theta = \frac{4C}{K}t \tag{2.9}$$

The final type of damping that we explore in this lab is turbulent damping. We use turbulent damping by strapping some foam pieces perpendicular to the face of the disk. Turbulent damping exerts a torque with the following form.

$$\tau_{\text{turb}} = C_t \operatorname{sgn}(\dot{\theta})|\dot{\theta}|^n \tag{2.10}$$

We can see that this is just a generalization of Eqns. 2.4 and 2.8. Coulomb damping is just $n = 0$, while viscous damping is $n = 1$. However, as we have $n > 1$ our differential equation becomes non-linear and thus very tricky to solve. In this case the log decrement decreases as the oscillation amplitude decreases, which is to say the oscillation decays "more slowly" as amplitude decreases. In the $n = 2$ case we can show that the log decrement follows the following relation.

$$\delta = \frac{8C}{3I}\theta_0 \tag{2.11}$$

Once we start using the motor and $\tau_{\text{ext}} \neq 0$ we have completely different solutions to the differential equation. These new external torques can be modeled by the following equation.

$$\tau = K\lambda\theta_0 \cos(\omega t) \ , \quad \lambda = \frac{L_1}{L_1 + L_2} \tag{2.12}$$

Solutions to these non-homogeneous differential equations are composed of two different parts: the transient and the steady state. The transient solutions are what we were just examining, the short term responses of the pendulum as it begins oscillating. The steady state solutions are the long term responses to the driving of the motor.

$$\theta_{\text{SS}} = B(\omega)\cos(\omega t - \beta(\omega)) \tag{2.13}$$

Where $B(\omega)$ and $\beta(\omega)$ are defined as follows.

$$B(\omega) = \frac{\lambda\omega_0^2\theta_0}{\sqrt{\left(\omega_0^2 - \omega^2\right)^2 + 4\omega^2 a^2}}\ , \quad \beta(\omega) = \arctan\left(\frac{2\omega a}{\omega_0^2 - \omega^2}\right) \tag{2.14}$$

Resonance is defined as the point where the amplitudes construct the most at a certain frequency. This occurs at the natural frequency, ω_0. The phase of the motor and the pendulum have some shift which is described by $\beta(\omega)$.

When scanning by frequency we can describe the width of the half-power points (points along the amplitude versus frequency plot that the amplitude has dropped by a factor of $1/\sqrt{2}$ by a constant γ.

$$\gamma = \frac{R}{I} = 2a \tag{2.15}$$

In addition to log decrement, all of our damped systems can be described by their quality factor, Q. This quality factor is defined as follows.

$$Q = \frac{\pi}{\delta} \tag{2.16}$$

Another concept with regards to driven oscillations comes from the phenomenon of beats. Beats come from measuring the sum of two harmonic signals with frequencies ω_1 and ω_2 as follows.

$$y_1 = A\sin(\omega t + \varphi_1)\ , \quad y_2 = B\sin(\omega t + \varphi_2) \tag{2.17}$$

We can define the beat frequency, β, as the following.

$$\beta_{1,2} = \frac{\varphi_1 \pm \varphi_2}{2} \tag{2.18}$$

In the case that the amplitudes of the two waves are the same and the two frequencies are close we can derive the following expressions to help us describe the resulting wave.

$$\omega = \frac{\omega_1 + \omega_2}{2} \approx \omega_{1,2}\ , \quad \Omega = \frac{\omega_1 - \omega_2}{2} \tag{2.19}$$

Giving us the following form for the waveform.

$$y = 2A\cos(\Omega t + \beta_2)\sin(\omega t + \beta_1) \tag{2.20}$$

However, since life is never easy, we have the solution where $A \neq B$.

$$y = C(t)\sin\left((\omega + \beta)t\right) \tag{2.21}$$

$$C(t) = \sqrt{A^2 + B^2 + 2AB\cos(\Omega t)} \tag{2.22}$$

$$\beta(t) = \tan^{-1}\left(\frac{B\sin(\Omega t)}{A + B\cos(\Omega t)}\right) + \begin{cases} 0, & A + B\cos(\Omega t) \geq 0 \\ \pi, & A + B\cos(\Omega t) < 0 \end{cases} \tag{2.23}$$

Finally, for driven oscillators we can look at sub-harmonics. It has been noticed that if one drives the oscillator at some integer multiple (or divided by some integer multiple) of the natural frequency, more complex motion is observed. This complex motion is the result of a non-linearity in the system.

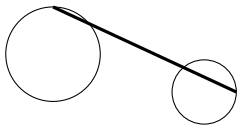

Figure 1: Sketch of motor used in our later experiments

The motor (sketched in Figure 1) has two circular wheels with a bar in between them. The circles rotate and move the bar, driving our system. The system is not driven exactly in a sinusoidal motion, sub-harmonics exacerbate the distortion.

Now that we have a good understanding of damping and how we are going to look at damping in this lab, let's consider situations that are undamped.

The first situation that we will consider is that of a mass on a wire hanging from our pendulum. We investigate this case because knowing the displacement of the pendulum with the mass attached allows us to calculate the torsional spring constant K.

Hanging each mass off the pendulum we observe that the displacement has a sort of "stair-step" pattern, we can look at the value of the displacement on each of these steps and plot them against the mass that we hang. Doing so should yield a straight line with the following slope.

$$\theta = \frac{g\rho}{K}m \tag{2.24}$$

Where g is the gravitational constant and ρ is the radius of the disk. Since we are finding the slope and its expression has only one unknown, we can determine the value of K from this.

Once we know K we can learn a great deal more about our system. Firstly, we can learn about the shear modulus, G, of the wires holding the disk. The shear modulus is the ratio of the shear stress and the shear strain. Its relationship with K is as follows for each of the i wires.

$$K = \frac{\pi G r^4}{2L_i} \tag{2.25}$$

In addition to the shear modulus we can also find the natural frequency of the pendulum. In Experiment 3.2 we use the torsion spring constant to solve for the frequency, but in Experiment 3.3 we do the opposite.

$$\omega_0 = \sqrt{\frac{K}{I}} \tag{2.26}$$

Where I represents the moment of inertia of our disk which is the product of the mass of the disk and its radius squared.

$$I = MR^2 \tag{2.27}$$

As always, Origin has a goofy parameter for its sine and sine damp functions w. The relationship between w and the frequency ω is as follows.

$$w = \frac{\pi}{\omega} \tag{2.28}$$

Finally we can find the percentage error on any of our values using the following equation.

$$\%\text{ error} = 100\left(\frac{|\text{expected} - \text{observed}|}{\text{expected}}\right) \tag{2.29}$$

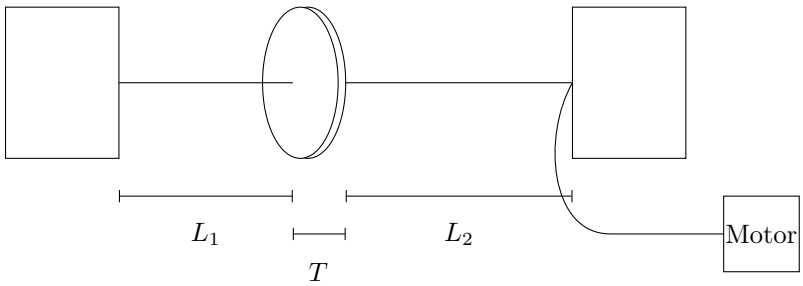

Figure 2: Basic Experimental Set-up

3 Experiment

3.1 Equipment

In this lab we used a number of different pieces of equipment (our set-up can be seen in Figure 2). We used two pieces of stainless steel piano wire (one of length 38 ± 1 cm other of length 36 ± 1 cm, each have thickness of 0.87 mm) to hold our torsional oscillator in place. The pendulum itself is just a metal disk with a hole in the center which allows the wires to pass. In order to track the rotation with any degree of accuracy we used a wheel with 1600 ticks attached to a buffer linked to our computer. On the computer we used a software that read the data from the buffer and displayed a plot for quality check and then outputted the data into a text file. In order to zero our pendulum and for damping in some experiments we used a large physical magnet that we could place around the disk to induce some force.

Additionally, we used a motor connected to an oscilloscope to drive the system in the later parts of the lab. The oscilloscope was also linked with the computer and controlled remotely with a software that allowed us to change the frequency, amplitude and duty cycle of the oscilloscope. For the entirety of the time we had the motor running we used a 5 V sine wave with duty factor set to 0%.

This experiment was conducted over two days and the second day we encountered an error with our set-up and changed lab stations. Below are the reported values for the mass, thickness and diameter of the disks we used.

Disk	Mass (g)	Diameter (cm)	Moment of Inertia[1](kgm^2)	Thickness (cm)
1	933.01 ± 0.1	10.142 ± 0.002	$2.39\times10^{-3} \pm 9.78\times10^{-7}$	1.324 ± 0.002
2	928.40 ± 0.1	10.162 ± 0.002	$2.39\times10^{-3} \pm 9.78\times10^{-7}$	1.324 ± 0.002

[1] Moment of Inertia from Eqn. 2.27

Table 1: Properties of the disks. Disk 1 used in §3.2 to 3.6, disk 2 used in §3.7 to the end.

We can neglect the disk and measurement device with the ticks linked to the computer in this because they are both low-mass and near the center of the disk. The low-mass means that it would not contribute meaningfully to the total mass anyway and it being near the center of the disk means that it would have even less of an effect on the moment of inertia.

As always data analysis for this lab was done in Origin Pro.

3.2 Determining the Torsional Constant from Static Measurements

For this part of the experiment we used the set-up in Figure 2 and we attach a wire along the thick side of the pendulum. We take the wire and add a masses to the end of it. We use masses of 5 and 20 g masses, starting with 5 and adding another 20 each time. Thus we get data on masses of 5, 25, 45, 65 and 85 g.

Adding these masses causes the system to rotate to and oscillate around a particular value. That value represents angular displacement that the mass moves the pendulum. This can be seen in the following figure.

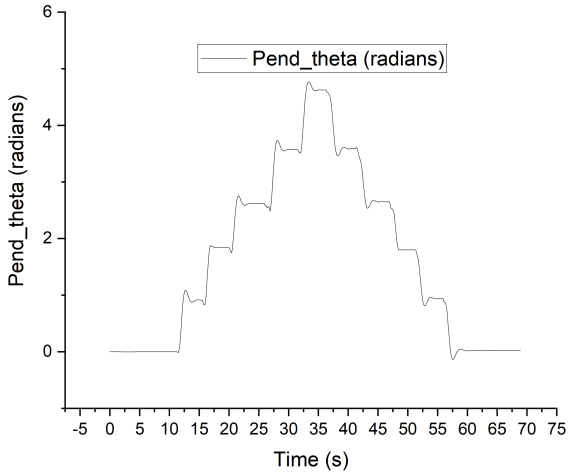

Figure 3: Plot of the displacement of the torsional pendulum with added masses versus time. Each 'step' here represents adding or taking off 20g

Mass (g)	5	25	45	65	85
Displacement (rad)	0.9142	1.84309	2.62234	3.57187	4.62342

Table 2: Each of the displacements of the disk by each of the masses (taken from steps doing up)

Knowing these displacements we can plot them against the mass. This should yield a straight line with slope described in Eqn. 2.24, where g and ρ are constants (gravitational constant and radius of disk, respectively). From this we can solve for the torsion spring constant K.

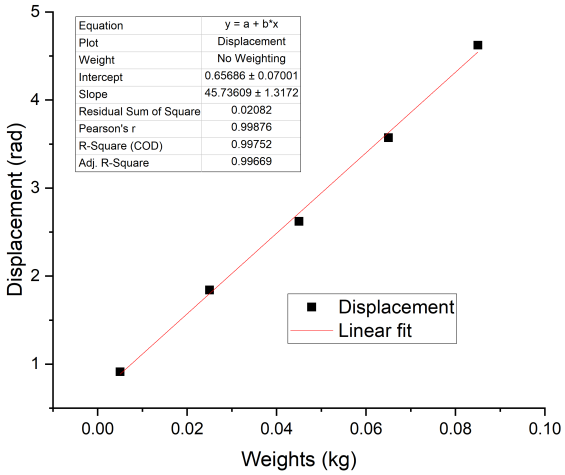

Figure 4: Linear relationship between the weights added in kg and the displacement in radians

We obtain a value of 45.736 ± 1.3172 for our slope. Using 9.81 for g and the radius of disk one in Table 1 corresponds to a torsional spring constant value of 0.01087 ± 0.0003 N m rad^{-1}.

From Eqn. 2.25 we can find G, the shear-modulus of the material, for the wires. We know that both wires are stainless steel which has a shear modulus of 77.2 GPa[2].

G_1 (GPa)	G_2 (GPa)
73.487 ± 2.866	69.619 ± 2.786

Table 3: Values for the shear-modulus for each of the wires (wire thickness 0.87 mm)

Based on our values from Table 3 we can calculate the percentage error (Eqn. 2.29) on each of our calculated values based on the value we looked up.

$$\%\text{error}_{G1} = 100\left(\frac{|73.847 - 77.2|}{77.2}\right) = 4.3\%$$

$$\%\text{error}_{G2} = 100\left(\frac{|69.619 - 77.2|}{77.2}\right) = 9.8\%$$

As we can see there is fairly good accuracy with our expected value of 77.2 GPa, meaning we can say with relative confidence that this is in fact stainless steal, as predicted.

There were a lot of steps leading up to the calculation of G, therefore small errors could have permeated through. One of these potential errors comes from our measurement of the 'equilibrium' value of the displacement by the masses. We basically just found a central value on the step and took that to be our value, certainly an average over the region could have yielded a more accurate value. This would effect our value for K and, consequently, our value for G. In addition the measurement of the length of the wire is based entirely off the total length of the system and the thickness of the disk. These values could have some slight deviation from reality and cause our values for G to be incorrect. Additionally, the masses are not measured particularly closely, we are just using the integer value printed on the mass and any deviation from this number would change our K and G.

Additionally, since we have the moments of inertia from Table 1 we can find the natural frequency of the pendulum using Eqn. 2.26. We end up with a value of $\omega_0 = 2.130 \pm 0.0307$ rad s^{-1}. We come back to this value when we compare this value against the fitted natural frequency in experiment 2.

3.3 Determining the Torsional Constant from Dynamic Measurements

For the second part of this lab we detached the wire and masses. In this section we considered only the free oscillations of the pendulum, which were just perturbed by a slight push by our TA Jordan.

We expect to see behavior that oscillations with a fairly constant amplitude at some frequency. This frequency will be the natural frequency, ω_0. Since we live in a non-perfect world the oscillations will decay due to some slight drag force exerted on it by the surrounding air.

[2] https://www.engineeringtoolbox.com/modulus-rigidity-d_946.html

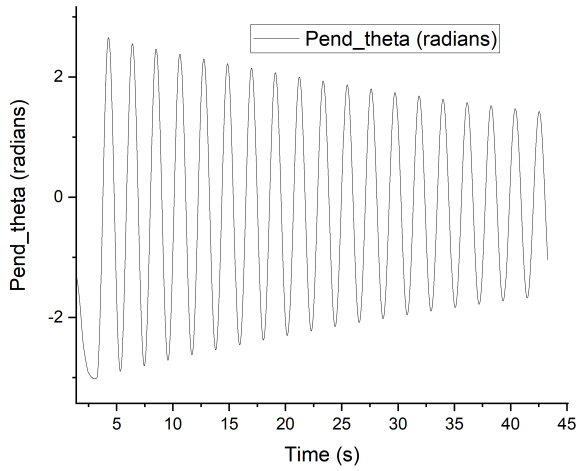

Figure 5: Free oscillation: angular displacement versus time

As expected we see the oscillations from peak to peak all have *roughly* the same amplitude with a general trend of decreasing, as expected. Next we fit the first couple of peaks in Origin with a sine function fit.

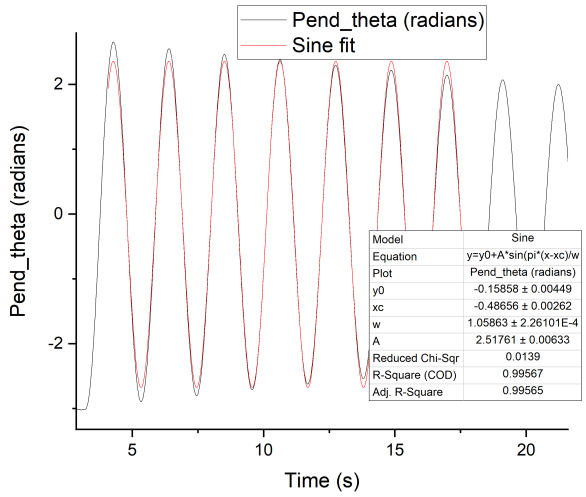

Figure 6: Free oscillation: fitting the oscillation with a sine curve

From this fit we obtained Origin's frequency parameter w as $1.0586 \pm 2.261\times10^{-4}$ s. Using Eqn. 2.28 we obtain a value of $2.965 \pm 6.326\times10^{-4}$ rad s^{-1} for ω_0.

One of the experimental errors on this measurement comes from this some unavoidable friction with the air we mentioned earlier. From this non-negligible effect our Origin fit is slightly inaccurate since it is not a perfect sine function that we are fitting.

Using our value for ω_0, Eqn. 2.26, and the moment of inertia value from Table 1 we can calculate the torsional spring constant K. We obtain a value of $0.0211 \pm 9.7020\times10^{-6}$.

We can compare the values of K and ω_0 of the free oscillation with what we got in §3.2

	K (Nm/rad)	ω_0 (rad/s)
Experiment 1	0.1087 ± 0.0003	2.130 ± 0.0307
Experiment 2	$0.211 \pm 9.702\times10^{-6}$	$2.965 \pm 6.326\times10^{-4}$

Table 4: Comparison of results for ω_0 and K in Experiments 1 & 2

As we can see there isn't great agreement within these two parameters; however, each of these values had its own experimental errors. The experimental errors impact the values differently and cause both of the values to stray from reality. The values are at least in the same general vicinity, therefore we can say confidently that both of these experiments follow the theory relatively closely.

3.4 Under- and Over- Damped Motion with Viscous Damping

The next experiment involved using the physical magnet to induce a damping force on our system. This damping is discussed in detail in the theory section. Essentially what we are doing in this experiment is taking a physical magnet and placing it around our disk. This causes the disk to have some decay, dependent on the amount of the disk inside the magnet.

The first case is under-damped, in this case we only put a little bit of the disk under the influence of the magnet. This causes the oscillations to decrease with a exponential envelope. This can be seen in the following figure.

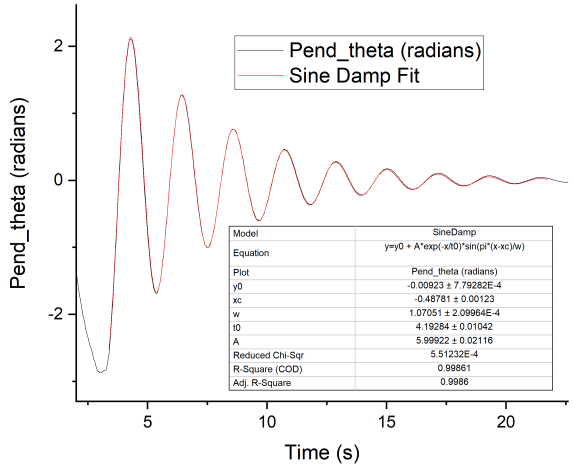

Figure 7: Example of under-damped motion, sine damp fit included

We can see that this decay envelope is exponential by looking at the value of the peaks. We plotted this and fit it to an exponential curve, shown in the following figure.

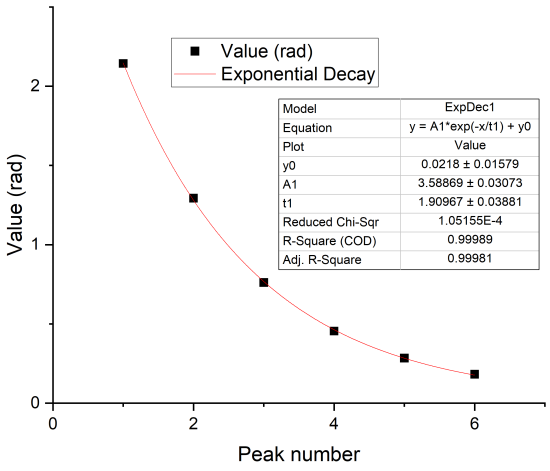

Figure 8: Plot of the peak values on the under-damped oscillations of the non-driven pendulum

From the fit in Figure 8 and Eqn. 2.6 that the attenuation constant a is 0.239 ± 0.00119.

Additionally, we can find the log decrement of the system, δ, fairly easily using the fit and Eqn. 2.7. We obtain a value of $0.5106 \pm 2.54\times10^{-3}$.

Finally, we can find the quality factor, Q, of the system, described in Eqn. 2.16. We obtain a value of 6.152 ± 0.0306 for the quality factor of our system.

a (s^{-1})	δ	Q
0.239 ± 0.00119	$0.5106 \pm 2.54\times10^{-3}$	6.152 ± 0.0306

Table 5: Summary of findings from under-damped situation

One of the errors we could have in these measurements is that we did not use Origin's peak finding routine, thus we hand picked the values for the peak, which could be off by some non-negligible amount. This would make our fit parameters for a and w different and would permeate through our other calculations.

The other situation that we observed was the over-damped case. In this case we place the magnet much further around the disk. This causes the oscillations to decay extremely quickly. In fact, this is how we zero the oscillations later in the lab. This quick decay can be seen in the following figure.

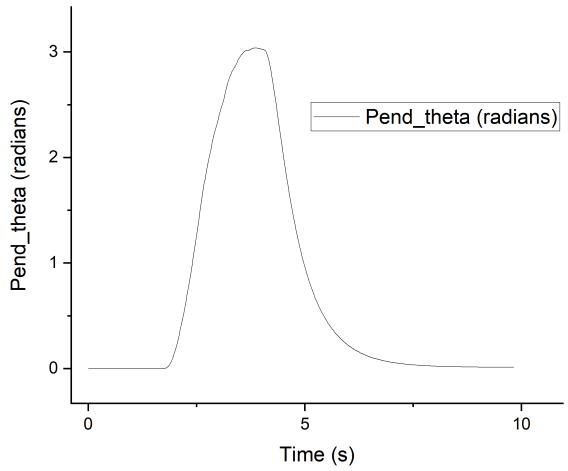

Figure 9: Plot of over-damped motion for our oscillator

As we can see, the damping does decay exponentially and rather quickly, making it a handy tool for zeroing the oscillations in the later sections of the lab

3.5 Coulomb Damping

For the next experiment we were looking at an extremely similar case as the previous experiment. This time instead of using a magnet to induce the damping force we will use a paint brush brushing against the thick side of the disk.

As described in the Theory section, this friction will cause the oscillations will decay with a linear envelope. This is because whenever the disk instantaneously stops to turn around the brush provides some static friction. As we can recall from any introductory physics course the coefficient of static friction will be higher than the coefficient of kinetic friction. This loss in energy to overcome the static friction causes the envelope to decrease linearly. In addition, this will cause the disk to not return exactly to the zero point.

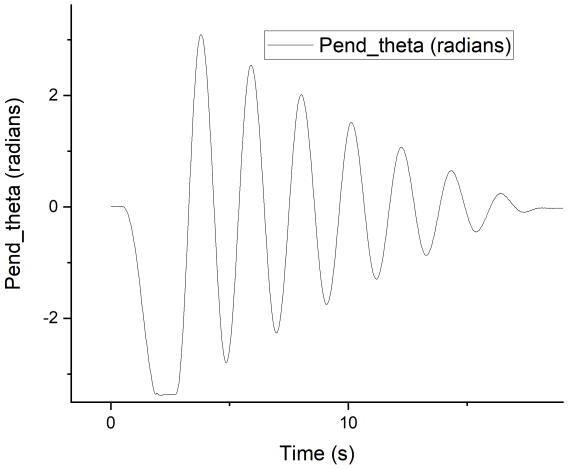

Figure 10: Example of Coulomb damping by a paintbrush. Notice the final displacement is greater than 0

We can find the frequency of the oscillations by looking at the peaks and finding the time it takes to go from one to the next. By inspecting the peaks we obtain a period of 2.10 ± 0.05 s, converting this to angular frequency using the normal relation we obtain $\omega = 2.992 \pm 0.0712$ rad s^{-1}. We can compare this value to the values we obtained for the natural frequency, ω_0, in experiments 1 & 2.

Experiment #	1	2	4
ω (rad/s)	2.130 ± 0.0307	2.965 ± 6.326×10^{-4}	2.992 ± 0.0712

Table 6: Comparison of angular frequencies across experiments 1, 2, and 4

The frequency of oscillations is roughly the same as in both experiments 1 and 2 (it has about the same amount of disagreement with the value from experiment 1 as experiment 2 does).

Additionally we can find the coulomb damping constant (C from Eqn. 2.8) looking at the slope of all of the peaks of the oscillations. This constant embedded in the slope of the line in Eqn. 2.9.

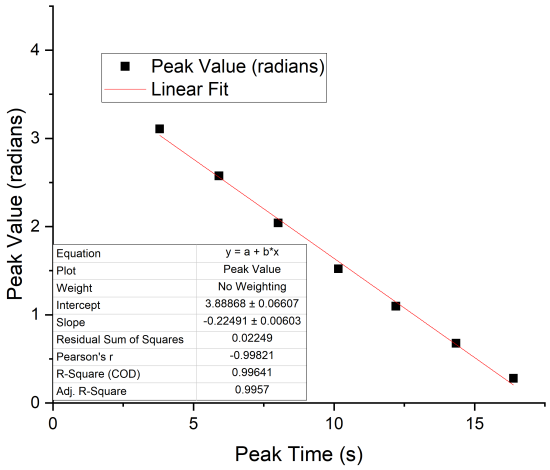

Figure 11: Peak values of the oscillations as a function of time

Here we can see the linear decay envelope quite clearly. The slope of this line is given as -0.22491 ± 0.00603. Using our two different calculated values of K in the first two experiments we can figure out where about this constant, C, should be.

C_1	C_2
-0.00611 ± 1.647×10^{-4}	-0.0119 ± 3.181×10^{-4}

Table 7: Two different estimates for C based on our tow different calculations of K

Similar to the viscous damping situation, we measured the peaks by hand. This shows up a little bit in the R values of our regression (not as close to 1 as we would like). Different values for the peaks could change the value of the slope and permeate through to the values for C.

3.6 Turbulent Damping

The next type of damping, and final experiment without driving our system with a motor, is turbulence. In this part we attached a couple small pieces of styrofoam perpendicular to the surface of the disk and then perturbed it.

The damping force is described by Eqn. 2.10 and is proportional to the velocity. This means that as it slows down the frictional force decreases. This effect causes the damping to decrease as the oscillations slow down. This effect yields an exponential decay, but different than in our viscous (magnetic) damping case.

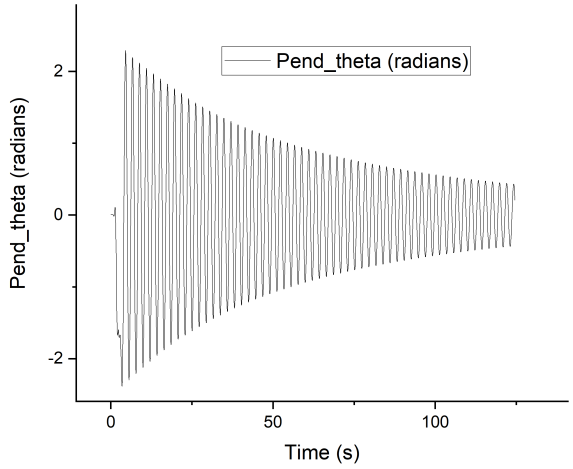

Figure 12: Turbulent Damping, notice how the decay takes an extremely long time, ~150s, to run down.

Using Origin's peak finder we can obtain all the values for the peaks on this long time interval. We can the calculate the log decrement of each successive peak by using Eqn. 2.5. Once we have found those values we plot the log decrement as a function of the amplitude in order to find the turbulent damping coefficient.

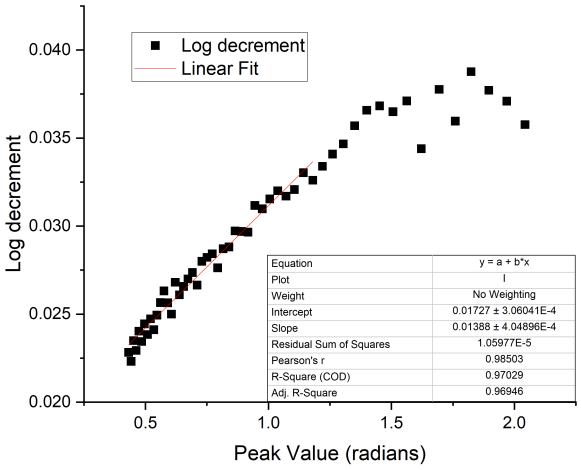

Figure 13: Log decrement as a function of amplitude, with a certain region fitted with a line

We can look at the plot in Figure 13 and determine an interval that the log decrement is linear on. Just based on the look of the graph we can estimate that log decrement versus amplitude is approximately linear out to around 1.25 radians (which corresponds to about $\pi/2.5$, which does not really hold any significant meaning). The value for the slope of this line is $0.0139 \pm 4.049\times10^{-4}$ and we can see that clearly the line tends towards the origin for smaller and smaller peak values.

This linear decay can be described with a log decrement similar to viscous damping, we can determine the decrement via the slope of the linear region of Figure 13. The equation of the line for this region is given by Eqn. 2.11, where I is the moment of inertia in Table 1. The slope, which we obtained in the fit of our data, allows us to calculate the damping coefficient C. We obtain $1.243\times10^{-5} \pm 3.629\times10^{-7}$ for the value of this constant.

A lot of the potential error on this value comes from where we decide the take the linear regression. It could be argued that we could start the linear regression around 1.5 radians which would decrease the radius and give us a completely different constant.

3.7 Phenomenon of Beats

This experiment is the first experiment including a driving motor, in addition any experiment beyond this point now refers to the second disk in Table 1. In this experiment we turn on the motor and then let the motor drive the oscillations of the pendulum back and forth. In addition we are using the physical magnet on this system so that amplitudes of the oscillations do not become so large as to break the wire.

As alluded to in the Theory section, once we let this system go the oscillations of the pendulum rise and decay with themselves a sinusoidal dependence. This effect is known as the phenomenon of beats and has to do with the phase difference of the oscillations of the pendulum with those of the motor. Here we drive the motor at a frequency of $f \approx 0.8 f_0 = 0.38024$ Hz and watch the disk oscillate at its natural frequency, $f_0 = 0.4753$ Hz (f_0 determined for the second disk by examining the free oscillations as in §3.3).

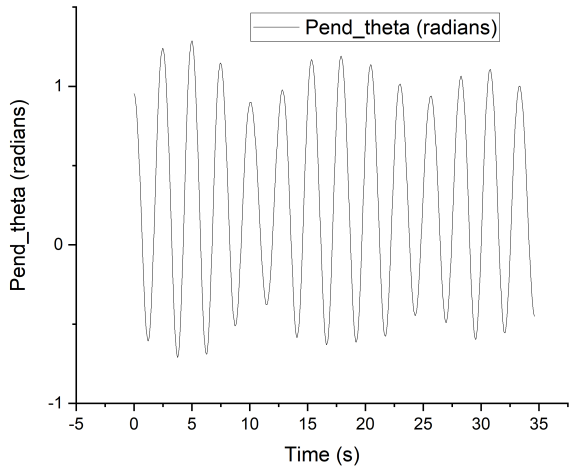

Figure 14: Superposition of transient and driven motion of our oscillator

The behavior in Figure 14 is as expected, the oscillations follow some sinusoidal envelope, representing the two different frequencies the system oscillates at.

We can take the fast-Fourier transform (FFT) of the oscillations to obtain the main frequencies that the system has. Now that we know the frequencies of both the envelope and the oscillations within, we can find the beat frequency using Ω in Eqn. 2.18.

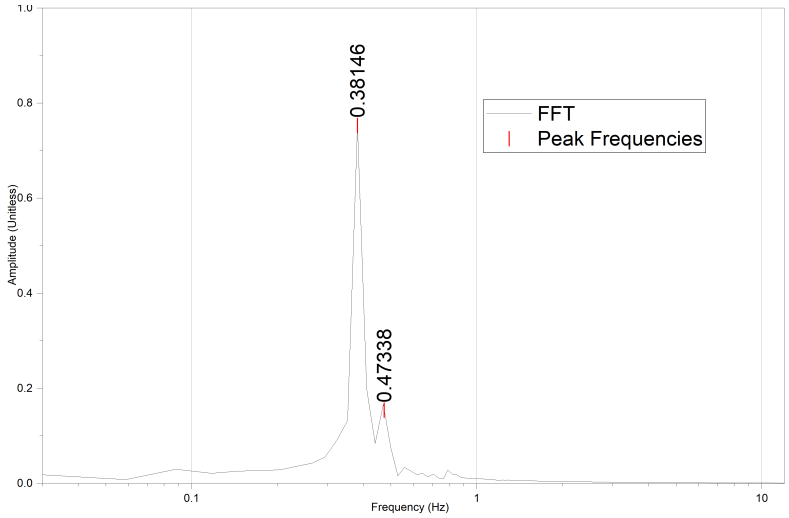

Figure 15: FFT of the oscillations, higher frequency corresponds to the frequency of oscillations while the lower one represents the frequency of the sinusoidal envelope

From Figure 15 we obtain the values of the frequencies to be 0.381 ± 0.004 Hz and 0.473 ± 0.004 Hz. These values are fairly close to the actual values of ω and ω_0. Thus, our experimental beat frequency was 0.2890 ± 0.0177 rad s^{-1}, while our expected value was 0.2873 rad s^{-1}. From these we can calculate our % error using Eqn. 2.29.

$$\%\text{error} = 100\left(\frac{|0.2890 - 0.2873|}{0.2873}\right) = 0.59\%$$

As we can see there is extremely close agreement with our expected values. This speaks to the effectiveness of the FFT. One experimental error that we could have encountered comes from the measurement of ω_0. We applied the same process as we did in experiment 2 (§3.3) and an error we had there was that the surrounding air did damp the oscillations slightly, thus our fit of a sine curve was technically wrong. Thus, our value for ω_0 could be off by some amount.

Although there is not a lot of error in our calculation some of it comes from our amplitude of the oscillation in Figure 14 never reaches some value and then stays there. It seems like we ran the computer program before the system reached a steady state after modifying the frequency. This clearly did not impact the results a whole lot, but it definitely impacts the results a little bit.

3.8 Measurement the Amplitude and Phase of Damped, Driven Oscillator

During the next part of the lab we are measuring the amplitude and phase of the oscillator as we vary the driving frequency. We use our physical magnet again to have some decay on our system as we perturb it so as to not have our amplitudes become too high and break the piano wire.

The first part of this experiment is extremely similar to that of experiment 3 (§3.4), where we perturb the oscillator and we want to measure the same things as before (attenuation constant, a, decay time, $1/a$, log decrement, δ, and Quality factor Q).

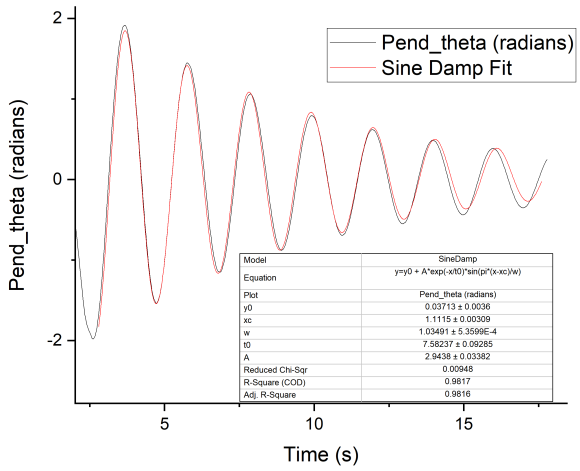

Figure 16: Non-driven oscillations of an under-damped system

From the fit in Figure 16 along with Eqns. 2.6 and 2.7 we can find all of our desired quantities.

a (s^{-1})	$1/a$ (s)	δ	Q
0.132 ± 0.0032	7.582 ± 0.093	0.273 ± 0.0067	11.509 ± 0.282

Table 8: Summary of values from non-driven, under-damped motion

When we vary the driving frequency we will observe some critical frequency that will have the largest response of the oscillator. This frequency will correspond to the natural frequency of the oscillator. We define driving the system at the natural frequency as resonance.

There are three different ways we can drive our oscillator: below, at or above resonance. Each of the are shown, in that order, in Figure 17

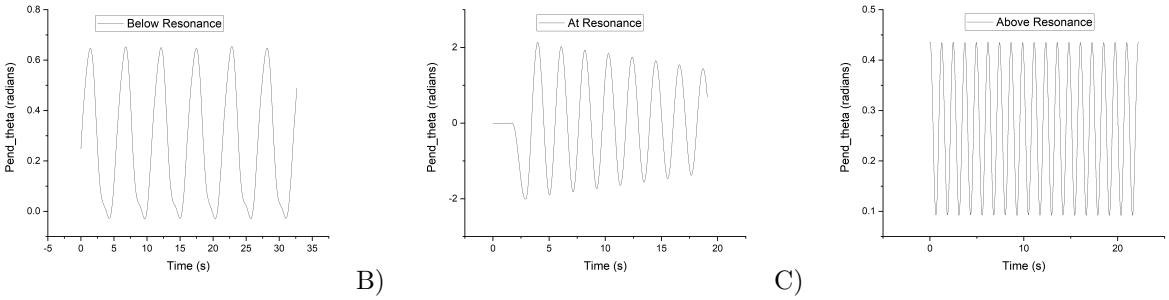

A) B) C)

Figure 17: Oscillator being driven A) Below resonance, B) at resonance, and C) above resonance

Now we can vary the frequency of the driving oscillator. We chose frequencies from 200 to 1300 Cal-out's which translates to 0.125 to 0.8125 Hz. Cal-out's is the unit of measure for the small plastic disk connected to the computer. 1600 Cal-out's corresponds to 360 degrees or 2π radians.

Varying the output allows us to examine the amplitude and phase response of our system as we move to and away from resonance.

First, we will look at the amplitude as a function a frequency. As we can see in the plots in Figure 17 we expect the amplitude to increase as it approaches resonance and then decrease as we get further from resonance.

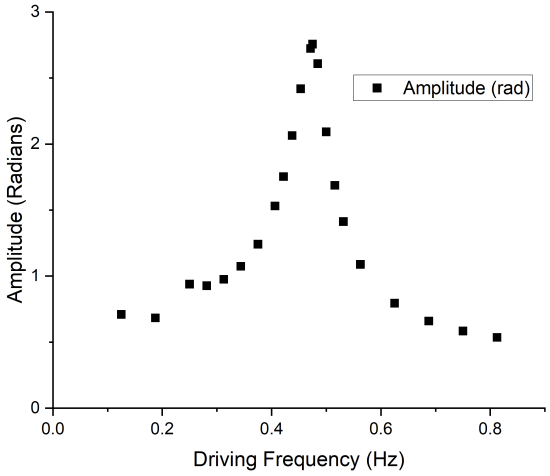

Figure 18: Amplitude of the oscillations as a function of frequency

Indeed we do see the trend as predicted. The maximum value of the amplitude is 2.756 radians, thus we expect the half-power points to be around 1.948 radians. The nearest two values are 2.064 radians at 0.4375 Hz and 2.092 radians at 0.5 Hz. Thus, based on our definition in the theory section, we can say that our γ = 0.0625 Hz. Recalling our relationship between the attenuation factor (a) and γ from Eqn. 2.15 we can say that a should be around 0.125. Referencing Table 8 we see that $a = 0.132 \pm 0.0032$ s^{-1}.

One of the main sources of error from this calculation of a comes from us not having full resolution of the amplitude versus frequency diagram. We had to estimate our half-power points with the next closest values, which were not particularly close, so our value for γ should actually be larger. If our γ we larger than it is easy to see that we would approach our actual value of a.

The next thing we looked at was the phase versus frequency diagram. The phase here is between the oscillator rotating and the motor driving it. When the oscillator is being driven it takes some time for the perturbation to travel down the line. Therefore, at large frequencies it would follow that the motor is going to be further out of phase with the disk, since it will be moving faster but the delay is still the same.

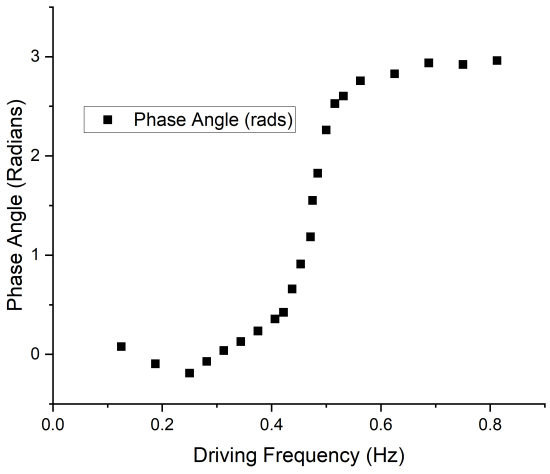

Figure 19: Phase difference of oscillator and motor versus frequency

The phase diagram follows as expected. When the phase is $\approx \pi/2$ we see a frequency of 0.475 Hz. This frequency makes complete sense because when the phase is 90 degrees (i.e. $\pi/2$ radians) out of phase the system is at the natural frequency. We measure the natural frequency of this system to be 0.4753 Hz. Therefore this result is as expected, as well.

Again, the resolution of our frequency scan limits our ability to accurately measure the value at the exact phase difference $\pi/2$. We were lucky, since we already knew what the value for the natural frequency of the system should be we were able to scan more finely around there as well as at the frequency itself.

3.9 Oscillator Driven at a Sub-harmonic of the resonant frequency

This experiment is very similar to the last experiment set-up wise, we have our oscillator which is underdamped and we drive it with the motor. We can drive the system at some so-called sub-harmonic of the resonant frequency. These sub-harmonics are the resonant frequency divided by some integer. One these sub-harmonics we observe similar behavior as to the resonant frequency only the magnitude is not quite as large.

As mentioned in the Theory section, these harmonics are caused by the (slightly) non-sinusoidal motions of the driving motor (see Fig 1 for visualization). We set the motor to $f = 0.23765$ Hz

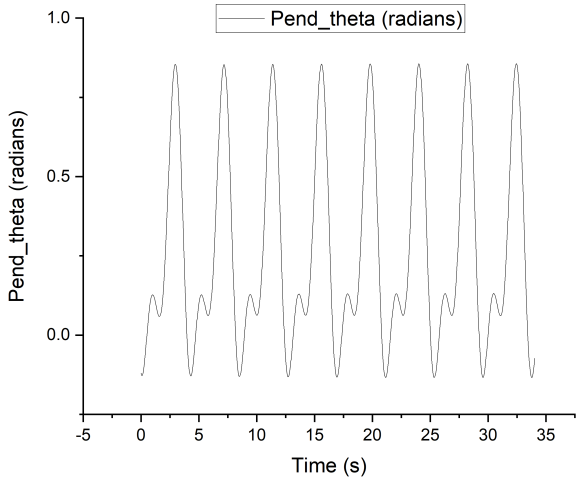

Figure 20: System driven at one-half the natural frequency

We can see this non-intuitive motion, caused by the motor driving the system at a sub-harmonic. The disk rotates to some angle and then comes back a little bit before rotating much further. This effect, again, is due to the response time of the pendulum on the wire. We can take the FFT of these oscillations so see the dominating frequencies.

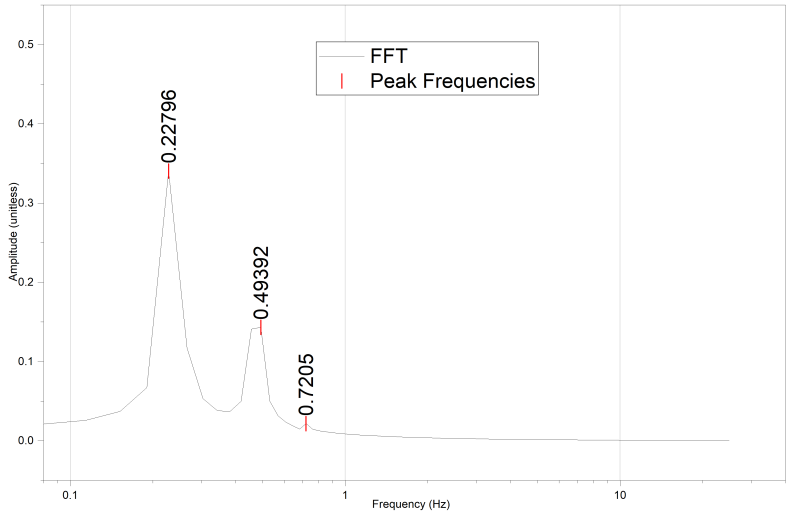

Figure 21: FFT with the values of the peak frequencies of the system

f_d (Hz)	$2f_d = f_0$ (Hz)	$3f_d$ (Hz)
0.22796 ± 0.004 Hz	0.49392 ± 0.004 Hz	0.7205 ± 0.004 Hz

Table 9: Values of peak frequencies of the driven system

From Table 9 we can see the values of the frequencies we obtain from the FFT in Figure 21. We can recognize these values as all pretty close to $f_0/2$, f_0, and $3f_0/2$. We can find the percent error of each of these values.

$$\%\text{error}_{f_d} = 100\left(\frac{|0.22796 - 0.23765|}{0.23765}\right) = 4.2\%$$

$$\%\text{error}_{f_0} = 100\left(\frac{|0.49392 - 0.4753|}{0.4753}\right) = 3.9\%$$

$$\%\text{error}_{3f_d} = 100\left(\frac{|0.7205 - 0.71295|}{0.71295}\right) = 1.05\%$$

As we can see, there is a pretty strong relationship between the expected values for the frequencies and the measured values. Some errors still persist. One of the sources of error from this experiment comes from the calculation of our natural frequency. We calculated the natural frequency in the same way as experiment 2 (§3.3), which we established in that discussion that method was not perfect. It is entirely possible that the measured natural frequency for that is inaccurate and our FFT reveals a more correct natural frequency. This could be one source of the discrepancies.

4 Conclusion

In conclusion, we can see that the rotational motions a disk attached on both faces by a wire are well described by our differential equation (Eqn. 2.1). For our homogeneous, non-damped solutions we saw a fair bit of agreement between our values for ω_0 and K. There were a couple of things that we could improve for these experiments in the future. Firstly, for the mass versus displacement experiment, in the future we should consider measuring the masses ourselves for further accuracy, as well as waiting more time and taking a time average of each 'step' on the plot. For the free oscillation experiment, perhaps attempting this experiment in a vacuum would help to eliminate as much unintentional drag as possible.

Similarly, we see really good following of theory with our homogeneous, damped experiments. Our viscous damping follows an exponential decay envelope with a roughly constant log decrement. The Coulomb damping case sees the linear decay envelope, as expected. Additionally, this damping type's frequency follows very closely with previous estimates of the natural frequency of the system. The final type of damped system we looked at was turbulent damping. For turbulence we saw that the decay was exponential, but instead of the log decrement being constant it increased linearly with amplitude, as expect. Overall, we had relative success achieving similar models as the theory for our homogeneous, damped situations. One small source of experimental error in these comes from our measurements from the small plastic disk connected to the computer. This disk only had 1600 notches on it, therefore it did not have perfect resolution of the pendulum theta. While getting more notches into the circle would certainly be difficult, getting the finer resolution would slightly help out our values for the amplitude. This effect would mostly show up in our analysis using the peak finder tool in Origin. Another small error that could cause the systems to be slightly more damped than we would expect is the friction with the air (all except experiment 5). As seen in Figure 5, over time the air will have some non-zero damping on the system. This will show up in both our viscous and Coulomb damping situations, too. Again, this will not present a large effect, but it still exists.

Finally, the last type of our differential equation is non-homogeneous. In the first of our non-homogeneous experiments, we examined the beat frequency of our system (run at $0.8f_0$). We saw that the oscillations followed some oscillatory envelope, as expected, that was dependent on our beat frequency. Additionally, once we calculated the beat frequency and compared to our theoretical value we saw great agreement here, too. Secondly, we ran a scan of frequencies on our motor to examine the amplitude and phase difference responses. Our data for the amplitude response, which predicted a peak amplitude at resonant frequency, follows our model wonderfully. We see similar results with the phase difference only with a little hick-up with the phase going negative for a brief moment. Finally, for our discussion of the sub-harmonic we see that our theory about the distortion due to our near-sinusoidal motor follows really closely with the observations. One of the largest sources of error for this section comes in the scan of frequencies. When computing the a parameters of the amplitude response, we do not have full resolution of the data. This lack of resolution (especially around the half-power points) creates a lot of error in our values for this part. In the future, a finer scan would help us eliminate a lot of this frustration. Another source of error comes from inspecting the maximum amplitude of Figure 14, we can see that the system did not quite reach steady state by the time we measured for the frequencies. This will cause some error on those measurements.